The 13th International Probabilistic Workshop (IPW2015)
University of Liverpool, UK, 4 – 6 November 2015

Numerical Stochastic Buckling Analysis of Structures with Randomly Distributed Geometrical and Material Imperfections

Marc Fina[1], Stefan Lauterbach[2] and Werner Wagner[3]

Institute for Structural Analysis, Karlsruhe Institute of Technology, 76131 Karlsruhe, Germany.
E-mail: marc.fina@kit.edu[1], stefan.lauterbach@kit.edu[2] and w.wagner@kit.edu[3]

In this paper, an in-depth assessment of buckling loads of structures with random material and geometrical imperfections is presented. A wide variety of methods for the simulation of Gaussian stochastic processes are available. Here, the Karhunen-Loève Expansion and the spectral representation method are used. In these methods, the correlation length controls the shape of the random field and hence the shape of imperfections, which has a significant influence on the buckling load. Thus, a parameter study is performed at different geometries: a steel plate under axial compression and a U-shaped cantilever beam. Additionally, the random imperfections can be computed for curved structures like a CFRP cylinder. For the assessment of the stochastic numerical model, the buckling load and shape is compared with the analytical solutions and experimental results. At last, the different impact of geometrical and material imperfections on the critical buckling load is recognized.

Keywords: Random Imperfections; Spectral Representation; Karhunen-Loève Expansion; Monte Carlo Simulation & Buckling Analysis of Shells

Introduction

In structural engineering, the need of thin-walled structures is becoming increasingly important. Especially in the automotive and aerospace industry, a lightweight design is used to save e.g. fuel. Because of the slim design, the loss of stability becomes more relevant and imperfections have a major impact on the critical buckling load. These imperfections can be variations of the nominal geometry or a spatial variability of the material parameters. Regulations are often not available for complex structures like cylindrical shells. Currently, the buckling load of a perfect structure has to be multiplied by a knock-down factor, which is determined in sophisticated experiments. Such a semi-empirical approach for isotropic and orthotropic cylindrical shells, which is still used, was published in 1965 by the National Aeronautics and Space Administration [Seide and Weingarten (1965)]. In the Eurocode 3 (DIN EN 1993), the standard for design and construction of steel structures, another conventional deterministic approach is proposed. Here, the material and geometrical imperfections should

The 13th International Probabilistic Workshop (IPW2015)
4 - 6 November 2015, University of Liverpool, UK
Edoardo Patelli & Ioannis Kougioumtzoglou (editors)

be taken into account in the form of critical eigenmodes with a specified amplitude for the FE-Model. Beside the accuracy in computing methods, a detailed representation of the imperfections for the numerical model is needed. Because of their random character, the spatial variation of uncertain geometric and material properties can be described by random fields. A first probabilistic approach is published by [Arbocz and Babcock (1991)]. There, the results of measurements of initial imperfections are represented in Fourier series and the Fourier coefficients are computed as random variables. Nowadays, the imperfections are treated as random fields for a more realistic description. From the wide variety of methods for the simulation of Gaussian stochastic fields, in this work, the spectral representation method from [Shinozuka, M. and Deodatis, G. (1991)] and the Karhunen-Loève Expansion (K-L) from [Loève (1977)] are used. In both methods a control parameter, well known as the correlation length, is available, which controls the shape of the random field. Also for a parameter study, the direct Monte Carlo Simulation (MCS) is used to simulate the stochastic buckling behaviour.

Generation of Random Imperfections by using Karhunen-Loève Expansion and Spectral Representation Method

There are two main types of stochastic fields: Gaussian or non-Gaussian. Most of the parameters in engineering systems are non-Gaussian, for example material (Young's modulus and Possion's ratio) or geometric parameters (thickness, the phase angles of the fibre alignment for composite materials, among others). But, due to the lack of experimental data the Gaussian approach is often used [Stefanou (2008)]. In this work, the Karhunen-Loève Expansion is used to compute the random geometrical imperfection and additionally the spectral representation method was selected to compute the random material imperfections. Both can be easily implemented in a Finite-Element-Code on element level.

The Karhunen-Loève Expansion

Based on the idea that a continuous random function can be represented by a complete set of deterministic functions with corresponding random coefficients, the K-L Expansion was introduced for representing a random field [Zhang and Ellingwood (1994)]. The series is given by

$$\boldsymbol{x} = \sum_{k=1}^{n} \boldsymbol{\varphi}_k(\hat{\boldsymbol{x}}) \, \sqrt{\lambda_k} \, \xi_k \tag{1}$$

where $\boldsymbol{x}$ describes the random field; $\boldsymbol{\varphi}_k$ and λ_k are the eigenfunctions and eigenvalues of the autocovariance function $C(\hat{\boldsymbol{x}}_i, \hat{\boldsymbol{x}}_j)$ with the position vector $\hat{\boldsymbol{x}} = [\hat{x}_1 \; \hat{x}_2]^T$. The variable ξ_k is the uncorrelated Gaussian random variable with zero mean and unit standard deviation. Because the last eigenvalues and eigenvectors have a low impact on the final random field, the series is usually truncated after k terms to save computing time [Stefanou and Papadrakakis (2007)]. Due to that, the vector of the eigenvalues has to be sorted by descending order.

$$\boldsymbol{\lambda} = [\lambda_1 \; \lambda_2 \; ... \; \lambda_n]^T \quad \text{with} \quad \lambda_1 \geq \lambda_2 \geq ... \geq \lambda_n \tag{2}$$

The 13th International Probabilistic Workshop (IPW2015)
4 - 6 November 2015, University of Liverpool, UK
Edoardo Patelli & Ioannis Kougioumtzoglou (editors)

Also, the K-L Expansion is a set of orthogonal deterministic functions, the eigenfunctions of the covariance and uncorrelated random variables. Therefore, the K-L Expansion can only be accomplished if the eigenvalues and eigenfunction of the covariance function are known. Hence, the covariance function must be predetermined. Here, an exponential form for a 2-D field is used from [Shang and Yun (2013)]

$$C(\hat{\boldsymbol{x}}_i, \hat{\boldsymbol{x}}_j) = \exp\left[-\frac{d(i,j)}{l_c}\right] = \exp\left[-\frac{\sqrt{(\hat{\boldsymbol{x}}_{1i} - \hat{\boldsymbol{x}}_{1j})^2 + (\hat{\boldsymbol{x}}_{2i} - \hat{\boldsymbol{x}}_{2j})^2}}{l_c}\right] \tag{3}$$

and in matrix notation

$$\boldsymbol{C} = \begin{bmatrix} C(\hat{\boldsymbol{x}}_1, \hat{\boldsymbol{x}}_1) & \cdots & C(\hat{\boldsymbol{x}}_1, \hat{\boldsymbol{x}}_n) \\ \vdots & \ddots & \vdots \\ C(\hat{\boldsymbol{x}}_n, \hat{\boldsymbol{x}}_1) & \cdots & C(\hat{\boldsymbol{x}}_n, \hat{\boldsymbol{x}}_n) \end{bmatrix} \tag{4}$$

where $d(i,j)$ is the distance between two nodes and l_c is the correlation length. Due to the symmetry of the covariance function, the covariance matrix is symmetric and positive definite. The correlation length controls how quickly the covariance falls off. For l_c tending to infinity or a zero distance between two separated points, the exponential covariance function converges to the value one, that means two points are full dependent. Otherwise, if the distance is greater than the correlation length, the points are nearly independent. The effect on the random field is shown in Fig. 1 for a square plate with 7×7 nodes. The shape becomes more uniform for great values of l_c. Often, engineering structures consist of many individual components. So, it is

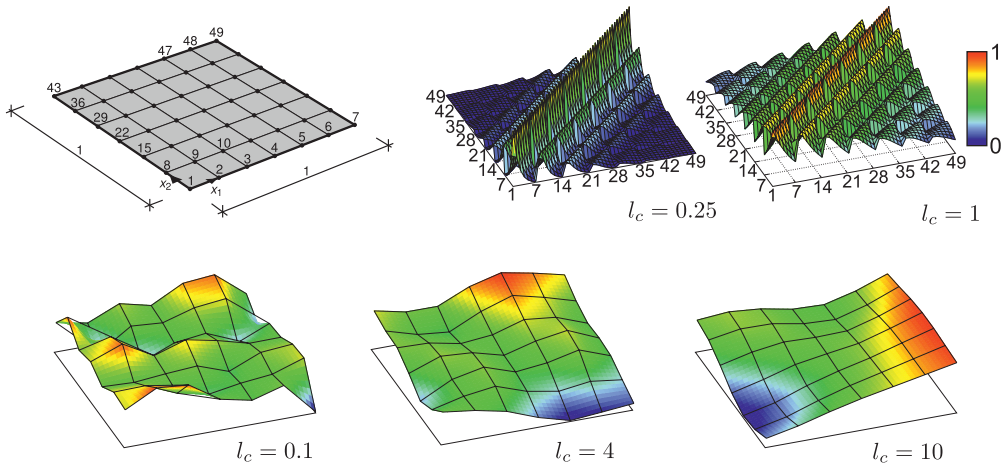

Fig. 1. Unconstrained covariance function and the final random field for different correlation lengths l_c.

necessary that some points of the random fields have a value of zero for their connection. This is possible with an adapted covariance matrix where the covariances of the relevant nodes are vanishing. For Gaussian random fields, this can be accomplished on the basis of

The 13th International Probabilistic Workshop (IPW2015)
4 - 6 November 2015, University of Liverpool, UK
Edoardo Patelli & Ioannis Kougioumtzoglou (editors)

a stochastic interpolation [Baitsch & Hartmann (2005)]. The constrained covariance matrix can be expressed as follows

$$\tilde{\boldsymbol{C}} = \boldsymbol{C} - \boldsymbol{B}\boldsymbol{A}^{-1}\boldsymbol{B}^{T} \tag{5}$$

where

$$\boldsymbol{A} = \begin{bmatrix} C(\tilde{\boldsymbol{x}}_1, \tilde{\boldsymbol{x}}_1) & \cdots & C(\tilde{\boldsymbol{x}}_1, \tilde{\boldsymbol{x}}_m) \\ \vdots & \ddots & \vdots \\ C(\tilde{\boldsymbol{x}}_m, \tilde{\boldsymbol{x}}_1) & \cdots & C(\tilde{\boldsymbol{x}}_m, \tilde{\boldsymbol{x}}_m) \end{bmatrix} \tag{6}$$

with the points $\tilde{\boldsymbol{x}}_1$, ..., $\tilde{\boldsymbol{x}}_m$ for which the covariance is known to delete and

$$\boldsymbol{B} = \begin{bmatrix} C(\hat{\boldsymbol{x}}_1, \tilde{\boldsymbol{x}}_1) & \cdots & C(\hat{\boldsymbol{x}}_1, \tilde{\boldsymbol{x}}_m) \\ \vdots & \ddots & \vdots \\ C(\hat{\boldsymbol{x}}_n, \tilde{\boldsymbol{x}}_1) & \cdots & C(\hat{\boldsymbol{x}}_n, \tilde{\boldsymbol{x}}_m) \end{bmatrix} \tag{7}$$

with the covariances of the unconstrained and constrained points. Now, for the example

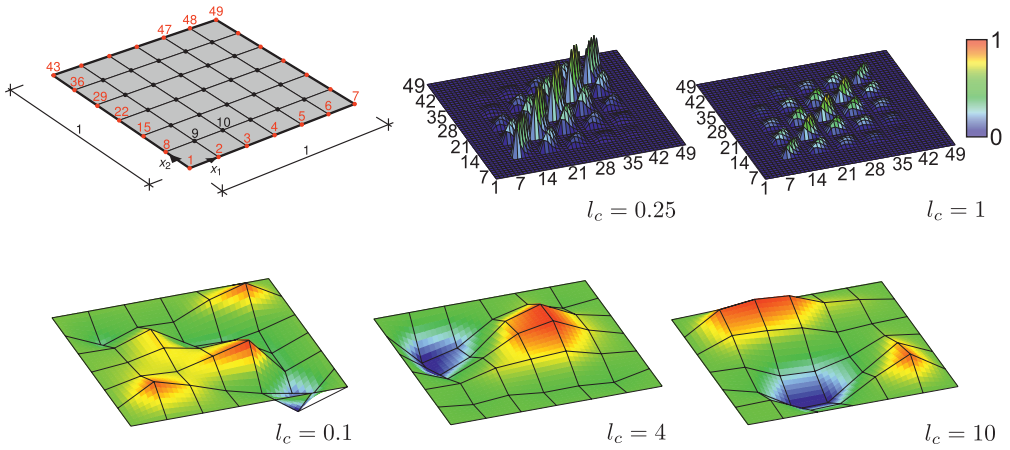

Fig. 2. Constrained covariance function and the final random field for different correlation lengths l_c.

the geometrical imperfections for the square plate should disappear on the edges. So the covariances of the 24 edge nodes have to be deleted. The result is a constrained and fitted covariance matrix with diagonal values smaller than one.

The Spectral Representation Method

The spectral representation method expands the multi-dimensional, homogeneous Gaussian stochastic field as a sum of trigonometric functions with random phase angles and amplitudes. The method is described in more detail by [Shinozuka and Deodatis (1996)] or [Stefanou

The 13th International Probabilistic Workshop (IPW2015)
4 - 6 November 2015, University of Liverpool, UK
Edoardo Patelli & Ioannis Kougioumtzoglou (editors)

and Papadrakakis (2007)]. Here, the formula for the simulation of a 2D-1V homogeneous stochastic field is used with the series of cosines

$$f^{(i)}(x_1,x_2)=\sqrt{2}\sum_{n_1=0}^{N_1-1}\sum_{n_2=0}^{N_2-1}\left[A^{(1)}_{n_1n_2}\cos\left(\kappa_{1n_1}x_1+\kappa_{2n_2}x_2+\phi^{(1)(i)}_{n_1n_2}\right)\right.$$
$$\left.+A^{(2)}_{n_1n_2}\cos\left(\kappa_{1n_1}x_1+\kappa_{2n_2}x_2+\phi^{(2)(i)}_{n_1n_2}\right)\right] \tag{8}$$

where $\phi^{(j)(i)}_{n_1n_2}, j=1,2$ are independent random phase angles distributed uniformly over the interval $[0,2\pi]$ for the (i) simulation. $A^{(1)}_{n_1n_2}, A^{(2)}_{n_1n_2}$ are defined as

$$A^{(1)}_{n_1n_2}=\sqrt{2S_{ff}(\kappa_{1n_1},\kappa_{2n_2})\Delta\kappa_1\Delta\kappa_2} \tag{9}$$

$$A^{(2)}_{n_1n_2}=\sqrt{2S_{ff}(\kappa_{1n_1},-\kappa_{2n_2})\Delta\kappa_1\Delta\kappa_2} \tag{10}$$

where

$$\kappa_{1n_1}=n_1\Delta\kappa_1;\qquad \kappa_{2n_2}=n_2\Delta\kappa_2 \tag{11}$$

$$\Delta\kappa_1=\frac{\kappa_{1u}}{N_1};\qquad \Delta\kappa_2=\frac{\kappa_{2u}}{N_2} \tag{12}$$

$$n_1=0,1,...,N_1-1;\qquad n_2=0,1,...,N_2-1 \tag{13}$$

$N_j, j=1,2$ are the numbers of trigonometric functions terms and $\kappa_{ju}, j=1,2$ are the upper cut-off wave numbers corresponding to the x_1 and x_2 axes in the space domain, which define the active region of the power spectrum $S_{ff}(\kappa_1,\kappa_2)$. This implies that the power spectral density function is assumed to be zero outside the region defined by

$$-\kappa_{1u}\le\kappa_1\le\kappa_{1u}\qquad -\kappa_{2u}\le\kappa_2\le\kappa_{2u} \tag{14}$$

The two-sided power spectral density function is given by

$$S_{ff}(\kappa_1,\kappa_2)=\frac{\sigma_f^2}{4\pi}b_1b_2\exp\left[-\frac{1}{4}(b_1^2\kappa_1^2+b_2^2\kappa_2^2)\right] \tag{15}$$

where σ_f is the standard deviation of the stochastic field and b_1, b_2 are the correlation parameters. A very important point is that the simulated stochastic field $f(x_1,x_2)$ is asymptotically Gaussian as the number of terms in the cosine series approaches infinity: $N_j\to\infty$, because of the central limit theorem. A popular aspect of the method is that the cosine series formula can be numerically computed very efficiently using the Fast Fourier Transform technique. In this method, the random field is often decomposed into a deterministic part and stochastic part as follows

$$\bar{f}(x_1,x_2)=\mu_0+f(x_1,x_2) \tag{16}$$

with the constant mean μ_0. It has to be taken into account that the mean of the random field $f(x_1,x_2)$ converges to zero only for great numbers of N_j. In Fig. 3 the random field is shown for a square plate with the dimension $1000\times1000\ mm$ and different correlation parameters. Here, the field becomes more uniform for great values of b_1 and b_2. Additionally, the waviness

The 13th International Probabilistic Workshop (IPW2015)
4 - 6 November 2015, University of Liverpool, UK
Edoardo Patelli & Ioannis Kougioumtzoglou (editors)

of the shape depending on the direction can be controlled by the choice of different correlation parameters.

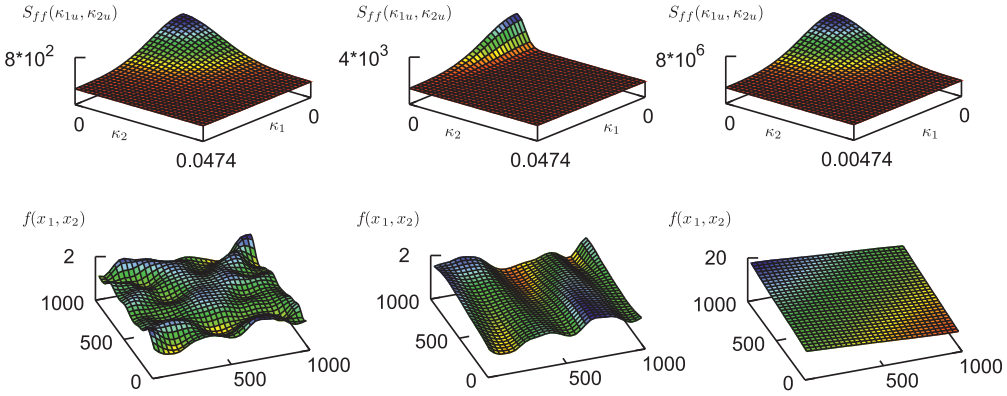

Fig. 3. Spectral representation with different cut-off wave numbers and correlation parametes: left: $b_1 = b_2 = 100\ mm$, centre: $b_1 = 100$, $b_2 = 500\ mm$ and right: $b_1 = b_2 = 1000\ mm$.

Monte Carlo Simulation (MCS) with a Nonlinear Quadrilateral Shell Element

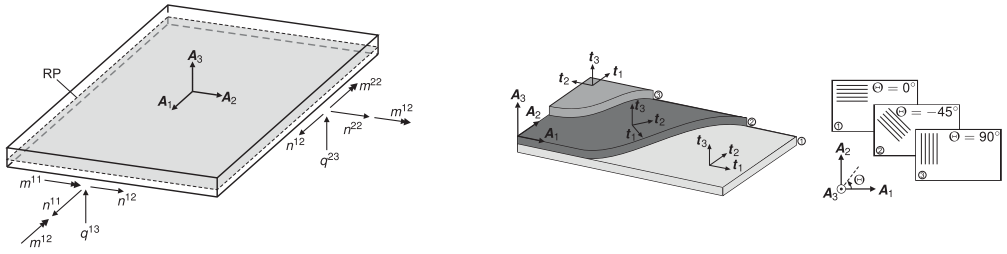

Fig. 4. Stress resultants on the reference plane (RP) and morphology of a layered material.

In this work a non-linear four-node isoparametric shell element with six nodal degrees of freedom (three global displacement and three global rotations at each node) from [Wagner and Gruttmann 2005] is used. To avoid shear locking, the assumed natural strain method (ANS) from [Dvorkin and Bathe 1984] is implemented. As well, for modelling composite laminates, the single-ply shell model is extended to a layered formulation with a freely selectable reference plane. The random deviations from the nominal geometry are described by initial nodal displacements of the Finite-Element-Mesh. This field of displacement must be read in before the finite-element calculation can be launched. Moreover, the random material properties like Youngs modulus, shear modulus and Poissons ratio are computed on element

The 13$^{\text{th}}$ International Probabilistic Workshop (IPW2015)
4 - 6 November 2015, University of Liverpool, UK
Edoardo Patelli & Ioannis Kougioumtzoglou (editors)

level of the shell formulation and in case of transversal isotropic layered materials, the change of layer thickness and fibre alignment can be taken into account.

Numerical Examples

The used shell element and the random material imperfections have been implemented in an extended version of the general finite element program FEAP [Taylor (2011)]. For the random geometrical imperfections a new external program was developed.

Axially Compressed Steel Plate

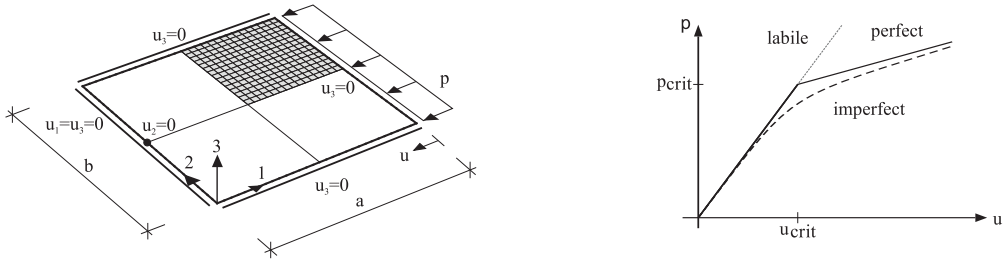

Fig. 5. Geometry and load-deflection curve of an axially compressed steel plate.

First, random geometrical imperfections are applied on an axially compressed steel plate ($E = 210\,000\,N/mm^2$, $\nu = 0.3$) with the thickness $t = 10\,mm$. Here, the aspect ratio $a/b = 1$ with $a = b = 1000\,mm$ is tested and the results of unconstrained and constrained imperfections are compared. For the FE-model 30×30 elements are used. The illustrated slab is simply supported. If the structure is loaded with imperfections, no distinct stability point occurs. Also a smooth equilibrium path occurs, which is shown in Fig. 5. Therefore, the critical displacement $u_{crit} = 0.362$ and load $p_{crit} = 798\,kN$ is calculated with an eigenvalue analysis of the perfect structure and then the imperfect plates are loaded by displacement control until the displacement u_{crit} is reached. According to Eurocode EN 1993 (EC 3) the first eigenmode as a critical imperfection is applied with an amplitude of $\Delta w = 5\,mm$. The FE-solution leads to a load of $540\,kN\,(0.72\,p_{crit})$. All buckling loads are normalized to p_{crit} and the Monte-Carlo-Simulation (MCS) includes 30 realisations. Fig. 6 shows that with an increasing correlation length the variance of the buckling loads decreases. The reason for that is caused by the Karhunen-Loève Expansion and the truncating of the series after k terms. That means that the sum of the series becomes smaller, thus also the amplitude of imperfection. To reverse the problem, the amplitude has to be scaled. Here, a scaling of $7\,mm$ is used as suggested by Eurocode. Now, the results for scaled imperfections (Fig. 7) show a greater variance. It can be concluded that the results of the constrained plate, where the imperfections of the edges are zero, have a smaller variance and the loads according to Eurocode 3 are on the safe side.

The 13th International Probabilistic Workshop (IPW2015)
4 - 6 November 2015, University of Liverpool, UK
Edoardo Patelli & Ioannis Kougioumtzoglou (editors)

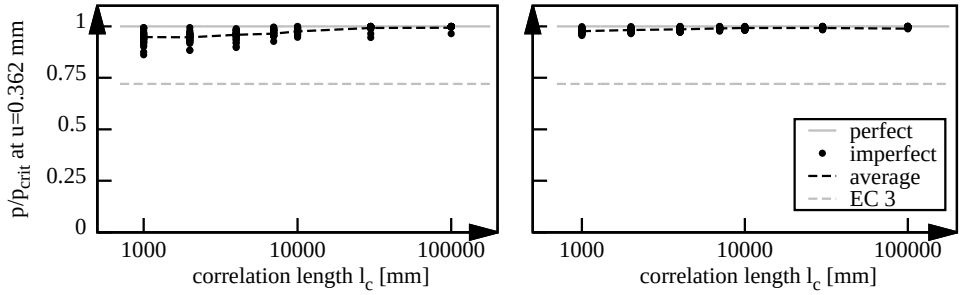

Fig. 6. Plate a/b=1: Load vs. correlation length (left: unconstrained and right: constrained) - unscaled.

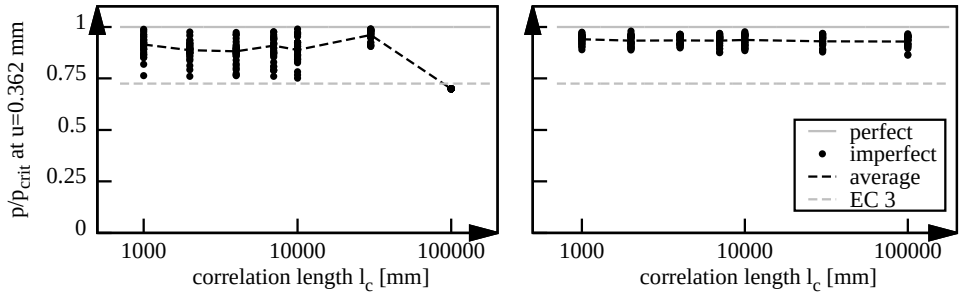

Fig. 7. Plate a/b=1: Load vs. correlation length (left: unconstrained and right: constrained) - scaled to an amplitude of 7 mm.

U-Shaped Cantilever Beam

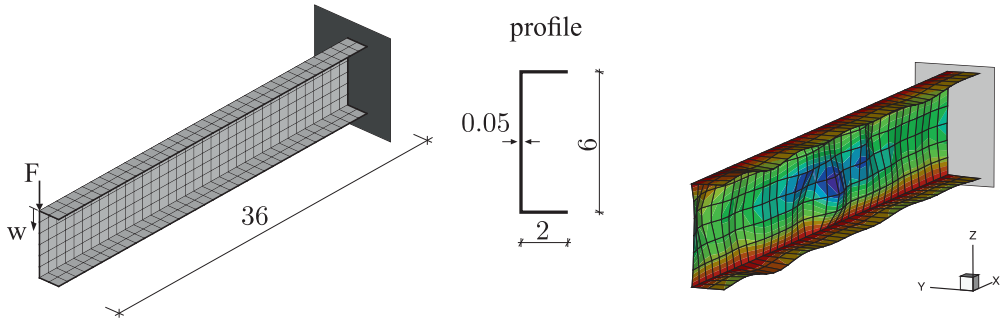

Fig. 8. Geometry and one selected random geometrical imperfection (50x enlarged) of the cantilever beam.

The 13th International Probabilistic Workshop (IPW2015)
4 - 6 November 2015, University of Liverpool, UK
Edoardo Patelli & Ioannis Kougioumtzoglou (editors)

The used stochastic methods can be applied to combined structures. Here, an U-shaped cantilever beam from [Chróścielewski et al.] is used. The material characteristics ($E = 1 \cdot 10^7$, $\nu = 0.333$) are dimensionless and for the FE-model 36 elements in length direction, 6 elements for the web and 2 elements for the flanges are selected. The beam is not loaded at the centre of shear, so torsional flexural buckling is the relevant mode of failure at $F_{crit} \approx 109$ and $w_{crit} \approx 0.2$. In this case the Eurocode 3 proposes two separate amplitudes for the critical eigenmode: $\Delta w_{\text{web}} = 0.03$ and $\Delta w_{\text{flanges}} = 0.01$, which also are used for scaling the imperfections, because no more detailed information is available. In Fig. 1 the sample of the random geometrical imperfections with the chosen correlation length $l_c = 360$ is shown. The stochastic fields of the three parts flange-web-flange are computed separately with respect to the constrained nodes. The buckling behaviour is studied for two different non-linear theories. Taking into account finite rotations (FR) a stiffening effect can be observed. For the simplification of moderate rotations (MR) the curve continues to decline after the critical point, so no lower bound can be detected. Therefore, this kinematic is used for the stochastic simulation. The results show that the load-displacement curve of the cantilever beam with the eigenmode as imperfection is no more the lower bound.

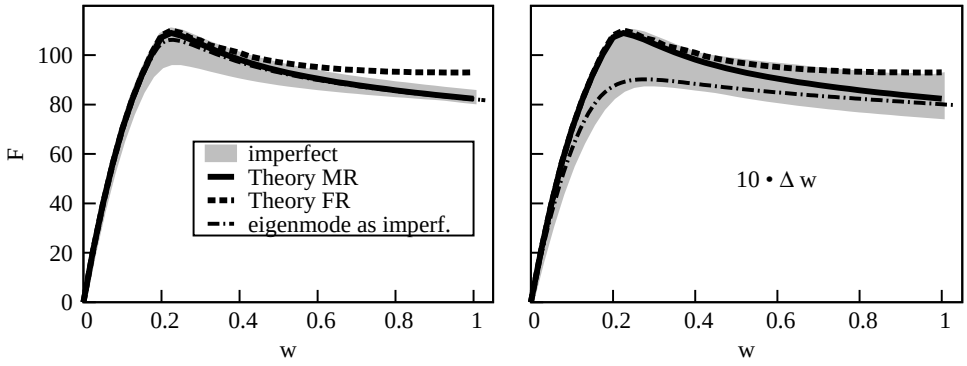

Fig. 9. U-shaped cantilever beam: load-displacement curve.

Composite Cylindrical Shell Z07

A fiber-compound cylinder, named Z07 from [Kriegesmann et al. 2010] is also considered as stochastic in its geometry and material. For the FE-Model 72 elements in circumferential direction and 24 elements in vertical direction are used. Furthermore the transversal isotropic material parameters and their stochastic characteristic have been obtained from [Degenhardt et al. (2007)]. The measured geometrical imperfections are served as the basis for the stochastic model. Here, an imperfection of around $3.2\,mm$ is picked out for the scaling and to achieve the similar shape. The correlation length of $20\,000\,mm$ is selected. For computing the stochastic field the cylinder is unrolled and the geodetic distance is used, see Fig. 10. Also for the

The 13th International Probabilistic Workshop (IPW2015)
4 - 6 November 2015, University of Liverpool, UK
Edoardo Patelli & Ioannis Kougioumtzoglou (editors)

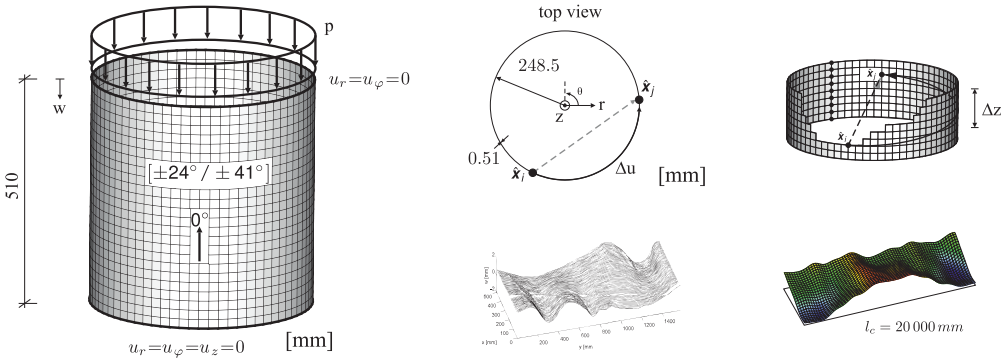

Fig. 10. Cylinder Z07: Geometry and Measurement of the geometrical Imperfections by [Kriegesmann et al. (2010)] with one selected stochastic imperfection ($l_c = 20\,000$).

constrained covariance function double nodes have to be deleted. Besides the deviation of the surface, the thickness and stiffness variation are computed with the spectral representation method. Therefore, the correlation is defined with respect to the length by the ratios b_i/L_i (thickness: $b_i/L_i = 0.35$ and stiffness: $b_i/L_i = 0.175$). To complete the stochastic model, the fibre alignment is also randomly distributed with a variance of $1.5\,\%$ of the mean. The graph in Fig. 11 shows that the results of the complete stochastic model are similar to the sample results from [Kriegesmann et al. (2010)] and to the empirical R-t curve from the NASA report [Seide and Weingarten (1965)]. Additionally, the right graph shows the different impact on the buckling load of all imperfections with the test data from [Hühne et al. (2008)]. In summary, the geometrical imperfections have a greater impact on the buckling load than the material variations.

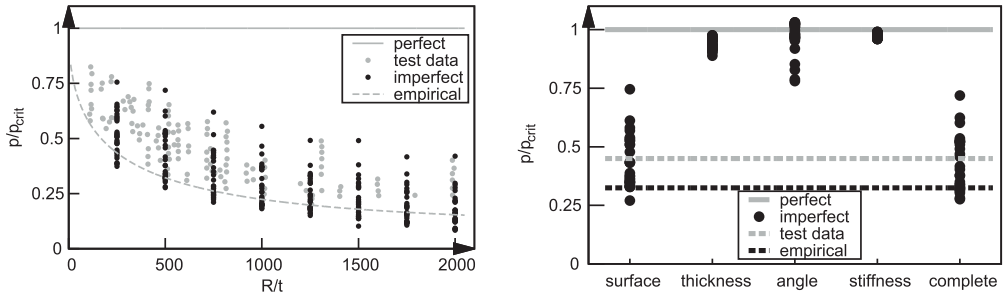

Fig. 11. R-t curve and summary of all imperfections of the cylinder Z07.

Conclusion

In this paper, the impact of generated random imperfections on the buckling load of isotropic and transversal isotropic shells is investigated. Not only the effect of geometrical deviations

The 13th International Probabilistic Workshop (IPW2015)
4 - 6 November 2015, University of Liverpool, UK
Edoardo Patelli & Ioannis Kougioumtzoglou (editors)

from the perfect shell structure but also the variability of Young's modulus, variations of the layer thickness and fibre alignment are considered. A study was carried out on the influence of the correlation parameter on the critical buckling load. Moreover, constrained random fields can be generated for assembly of combined structures like the U-shaped cantilever beam. Additionally, taking into account the geodetic distance for the correlation function, curved structures can also be simulated. Looking at the critical buckling load, the geometrical imperfections have a greater impact than the material ones. Summarized, the results of the stochastic simulations show a good correlation with experimental data. This work is one step to a stochastic overall model to present a better forecast of a lower bound of critical buckling loads, which are often stated too high in standards. Based on the great impact of the imperfection shape it is necessary to have more information on the influence of the correlation parameter.

References

1. Seide, P. & Weingarten V.I. (1965). Buckling of thin-walled circular cylinders, NASA/SP-8007. Space Vehicle Design Criteria (Structures).
2. Arbocz, J. & Ho, J.M.A.M. (1991). Collapse of axially compressed cylindrical shells with random imperfections. AIAA journal. 29(12), p. 2247-2256.
3. Shinozuka, M. & Deodatis, G. (1991). Simulation of stochastic processes by spectral representation. Applied Mechanics Reviews. 44(4), p. 191-204.
4. Loève, M. (1977). Probability theory. Springer Verlag N.Y.
5. Stefanou, George. (2008). The stochastic finite element method: Past, present and future, Comput. Methods Appl. Mech. Engrg. 198, p. 1031-1051.
6. Zhung, J. & Ellingwood, B. (1994). Orthogonal Series Expansion of Random Fields in Reliability Analysis, J. Engs. Mech. 120, p. 2660-2677.
7. Stefanou, G. & Papadrakakis, M. (2007). Assessment of spectral representation and Kahunen-Loève expansion methods for the simulation of Gaussian stochastic fields, Comput. Methods Appl. Mech. Engrg. 196, p. 2465-2477.
8. Shang, S. & Yun, G.J. (2013). Stochastic finite element with material uncertainties: Implementation in a general purpose simulation program. Finite Elements in Analysis and Design 64, p. 65-78.
9. Baitsch, M. & Hartmann, D. (2005). Optimization of slender structures considering geometrical imperfections. Inverse Problems in Science and Engineering 14(6), p. 623-637.
10. Shinozuka, M. & Deodatis, G. (1996). Simulation of multi-dimensional Gaussian stochastic fields by spectral representation 49(1).
11. Wagner, W. & Gruttmann F. (2005). A robust non-linear mixed hybrid quadrilateral shell element. International Journal for Numerical Methods in Engineering 64, p. 635-666.
12. Dvorkin, E.N. & Bathe, K.-J. (1984). A continuum mechanics based four-node shell element for general non-linear analysis. Engineering Compution 1(1), p. 77-88.
13. Kriegesmann, B., Rolfes, R., Hühne, C., Temer, J. & Arbocz, J.(2010): Probabilistic design of axial compressed composite cylinders with geometric and loading imperfections. International Journal of Strucutral Stability and Dynamics 10, p. 623-644.
14. Chróścielewski, J., Makowski, J. & Stumpf, H. (1992): Genuinely resultant shell finite elements accounting for geometric and material non-linearity. International Journal for Numerical Methods in Engineering 35(1), p. 63-94.
15. Degenhardt, R., Kling, A., Klein, H., Hillger, W., Goetting, H. C., Zimmermann, R., Rohwer, K. & Gleiter, A. (2007): Experiments on buckling and postbuckling of thin-walled CFRP structures using

advanced measurement systems. International Journal of Structural Stability and Dynamics 7(02), p. 337-358.
16. Hühne, C., Rolfes, R., Breitbach, E. & Temer, J. (2008): Robust design of composite cylindrical shells under axial compression - Simulation and validation. Thin-walled Structures 46, p. 947-962.
17. Taylor, R. (2011): Feap user manual, http://www.ce.berkeley.edu/projects/feap/manual.pdf.